A Non-apoptotic Function of MCL-1 in Promoting Pluripotency and Modulating Mitochondrial Dynamics in Stem Cells

Megan L. Rasmussen,[1] Leigh A. Kline,[1] Kyungho P. Park,[1] Natalya A. Ortolano,[1] Alejandra I. Romero-Morales,[1] Christin C. Anthony,[1] Kathryn E. Beckermann,[3] and Vivian Gama[1,2,*]

[1]Department of Cell & Developmental Biology, Vanderbilt University, PMB407935, 465 21st Avenue South, 4150A, Nashville, TN 37240-7935, USA
[2]Vanderbilt Center for Stem Cell Biology, Vanderbilt University, Nashville, TN 37240, USA
[3]Division of Hematology/Oncology, Vanderbilt University Medical Center (VUMC), Nashville, TN 37240, USA
*Correspondence: vivian.gama@vanderbilt.edu
https://doi.org/10.1016/j.stemcr.2018.01.005

SUMMARY

Human pluripotent stem cells (hPSCs) maintain a highly fragmented mitochondrial network, but the mechanisms regulating this phenotype remain unknown. Here, we describe a non-cell death function of the anti-apoptotic protein, MCL-1, in regulating mitochondrial dynamics and promoting pluripotency of stem cells. MCL-1 is induced upon reprogramming, and its inhibition or knockdown induces dramatic changes to the mitochondrial network as well as loss of the key pluripotency transcription factors, NANOG and OCT4. Aside from localizing at the outer mitochondrial membrane like other BCL-2 family members, MCL-1 is unique in that it also resides at the mitochondrial matrix in pluripotent stem cells. Mechanistically, we find MCL-1 to interact with DRP-1 and OPA1, two GTPases responsible for remodeling the mitochondrial network. Depletion of MCL-1 compromised the levels and activity of these key regulators of mitochondrial dynamics. Our findings uncover an unexpected, non-apoptotic function for MCL-1 in the maintenance of mitochondrial structure and stemness.

INTRODUCTION

Considerable efforts have been made to identify the gene networks that regulate the pluripotent state and control the first steps of differentiation, when cells start to acquire a cell-lineage-specific identity. These studies have identified key transcriptional regulatory networks that determine the pluripotent state (Kumar et al., 2014). In contrast, we know relatively little about how different organelles, such as mitochondria, adapt to the changing environments they encounter during differentiation and reprogramming. While increased mitochondrial fragmentation is a fundamental feature of reprogramming (Prieto et al., 2016), the molecular mechanisms underlying this phenomenon are not fully understood.

The mitochondrial dynamics machinery is composed of dynamin superfamily guanosine triphosphatases (GTPases) that have roles in either fission (division) or fusion of mitochondria. Dynamin-related protein 1 (DRP-1) is required for mitochondrial fission. DRP-1 activation is mediated in part by phosphorylation, ubiquitination, and sumoylation, which allow for increased recruitment to various receptors (e.g., FIS1) (Wai and Langer, 2016). However, these mechanisms of enhanced DRP-1 recruitment to the outer mitochondrial membrane are not well characterized in pluripotent stem cells (PSCs), where they appear to be constitutively active. Once activated, DRP-1 forms oligomers and assembles into rings that constrict around the mitochondria, dividing the organelle into separate entities (Westermann, 2010).

Fusion is mediated through the activity of the optic atrophy type 1 (OPA1) GTPase at the inner mitochondrial membrane and of mitofusins (MFN1 and MFN2) at the outer mitochondrial membrane (Chen and Chan, 2010). Mitochondrial dynamics is beginning to emerge as a crucial factor in regulating cell fate (Khacho et al., 2016; Longo and Archer, 2013; Martinou and Youle, 2011).

Many connections between the mitochondrial dynamics machinery and apoptosis have been made. Apoptosis is mediated by the BCL-2 family of proteins (Llambi et al., 2011). When cells are subjected to stress, the mitochondrial network has been shown to undergo DRP-1- and FIS1-mediated fragmentation in a process involving BAX translocation and co-localization with DRP-1 and endophilin B1 (Friedman and Nunnari, 2014; Karbowski et al., 2002; Sheridan et al., 2008). Previous reports suggested that BAX and BAK could also influence MFN2 function in healthy cells (Karbowski et al., 2006). The data shown in this report demonstrate that an anti-apoptotic protein belonging to the BCL-2 family, myeloid cell leukemia 1 (MCL-1), is a fundamental regulator of mitochondrial dynamics in human PSCs (hPSCs), independent of its role in apoptosis. MCL-1 is essential for embryonic development and for the survival of various cell types (Rinkenberger et al., 2000). Interestingly, recent studies have proposed that MCL-1 may also drive changes in cancer cell metabolic profiles to promote the biosynthesis of substrates needed for proliferation (Andersen and Kornbluth, 2012; Opferman, 2015).
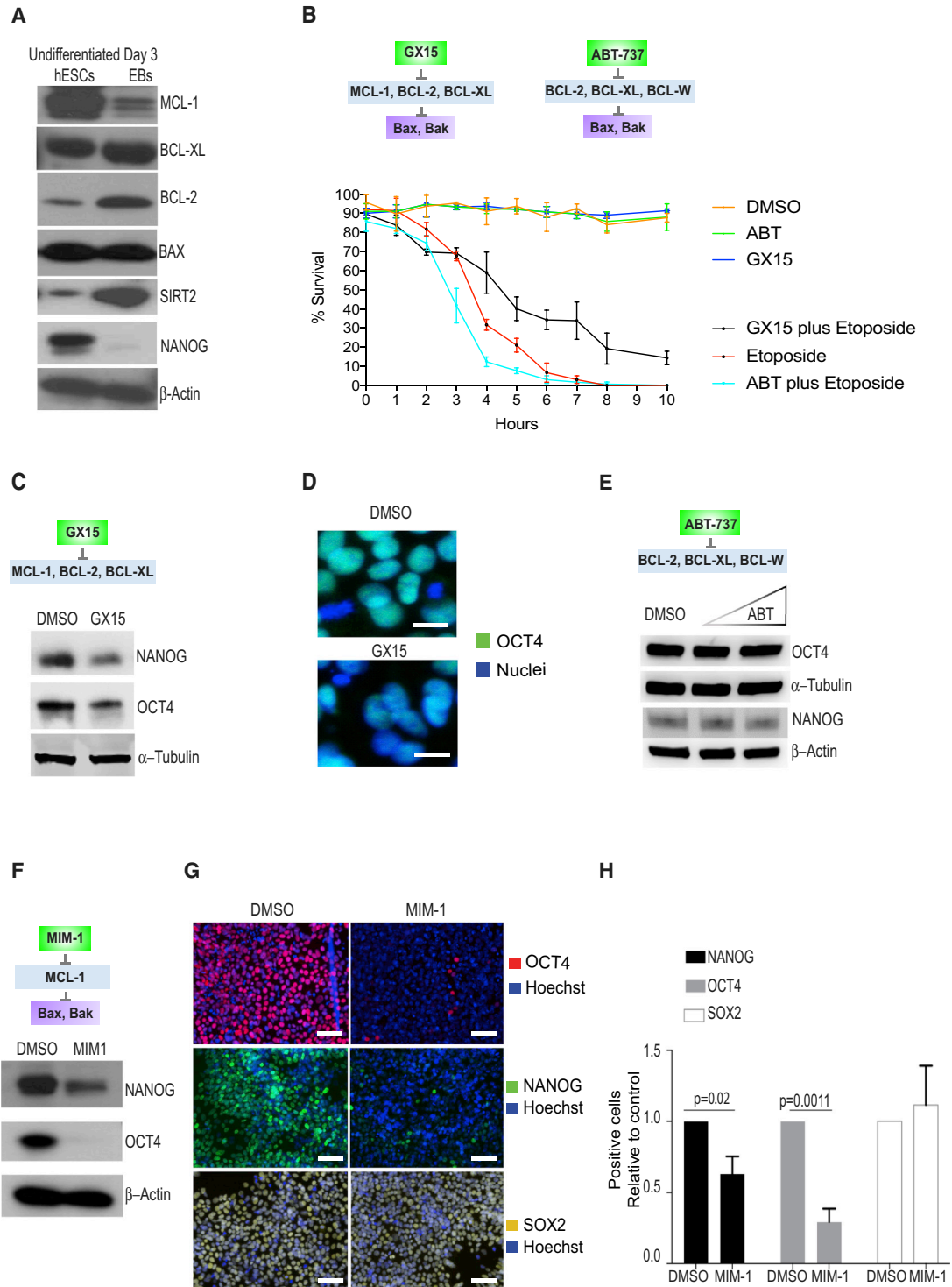
Figure 1. hESCs Engage Rapid Apoptosis after DNA Damage, which Can Be Reversed upon Cell Differentiation by MCL-1 Down-regulation

(A) MCL-1 protein expression is significantly decreased in EBs.

(B) hESCs were treated with GX15-070 or ABT-737 ± 20 μM etoposide. Cell survival was quantified each hour after etoposide treatment.

(C) GX15-070 treatment of hESCs results in decreased expression of NANOG and OCT4.

(legend continued on next page)

To examine the function of MCL-1 in both undifferentiated and differentiated cells, we took advantage of various features of the hPSC model, including (1) high expression of MCL-1, (2) a predominantly fragmented mitochondrial network, and (3) the ability to induce differentiation into early progenitor stages. This model provided an ideal system to examine not only the potential role of MCL-1 in mitochondrial structure but also its effects on cell fate. Here, we report MCL-1 as a modulator of mitochondrial dynamics in PSCs and demonstrate the value of the stem cell model in studying the plasticity of the mitochondrial network during reprogramming and differentiation.

RESULTS AND DISCUSSION

Human Pluripotent Stem Cells Downregulate MCL-1 upon Differentiation

We previously reported that human embryonic stem cells (hESCs) become resistant to DNA damage as differentiation is engaged (Dumitru et al., 2012). This resistance is in part associated with changes in the activation status of BAX, as well as mitochondrial priming (Dumitru et al., 2012; Liu et al., 2013). We first sought to probe the status of the apoptotic machinery by measuring levels of various BCL-2 family members during differentiation, when this apoptotic resistance is acquired. hESC colonies were grown in suspension in the absence of a matrix layer as aggregates, also known as embryoid bodies (EBs) (Odorico et al., 2001). We compared protein expression between hESCs and 3-day EBs by western blot analysis. Since differentiation causes apoptotic resistance, we expected to detect an overall increase in the expression of anti-apoptotic proteins and a decrease in the expression of pro-apoptotic proteins. As expected, the pluripotency transcription factor NANOG was downregulated in EBs, and sirtuin-2 (SIRT2), a NAD+-dependent deacetylase, which is induced upon differentiation (Ramalho-Santos et al., 2002), was upregulated. BAX and BCL-XL showed no detectable changes in expression during differentiation, and BCL-2 was significantly upregulated. In stark contrast, MCL-1 was significantly downregulated after only 3 days of differentiation (Figure 1A). MCL-1 downregulation was also detected in mouse ESC-derived EBs (Figure S1A). As reported previously, these results indicate that BCL-2 may be critical mediator of cell death

resistance in early differentiation (Liu et al., 2013). Counterintuitively, MCL-1 does not appear to be a major determinant of the apoptotic resistance characteristic of EBs (Dumitru et al., 2012).

To determine whether downregulation of MCL-1 was a particular trait of EB formation, we differentiated hESCs into trophoblast-like cells by addition of bone morphogenetic protein 4 (BMP4) and into neural progenitor cells using dual SMAD inhibition, as previously reported (Amita et al., 2013; Chambers et al., 2009) (Figures S1B–S1F). Differentiation to both lineages was accompanied by a significant downregulation of MCL-1 (Figures S1C and S1D), mimicking the EB formation results. This was unexpected, since EBs, trophoblast-like cells, and neural progenitor cells are more resistant to apoptosis than undifferentiated stem cells (Figures S1E and S1F).

To probe whether the downregulation of MCL-1 had a functional role in maintaining pluripotency, we examined the effect of inhibiting MCL-1 in hESCs. Cell-permeable, selective small-molecule antagonists of BCL-2, BCL-XL, and MCL-1, known as BH3 mimetics, have been identified (Ni Chonghaile and Letai, 2008). We first used the pan-BCL-2 inhibitor GX15-070 (Chiappori et al., 2012), which inhibits BCL-2, BCL-XL, and MCL-1, and compared it with the BH3-only mimetic ABT-737 (Oltersdorf et al., 2005), which only inhibits BCL-2 and BCL-XL. Since these small-molecule inhibitors target the main anti-apoptotic proteins, we expected treatment with etoposide in combination with either inhibitor to accelerate cell death onset compared to treatment with only etoposide. Not surprisingly, treatment with ABT-737 increased the sensitivity of hESCs to etoposide-induced DNA damage (Figure 1B). However, rather unexpectedly, treatment with GX15-070 had the opposite effect and resulted in reduced cell death sensitivity in response to etoposide (Figure 1B), pointing to a paradoxical effect of MCL-1 inhibition in mediating apoptotic resistance.

These results, together with the observed reduced MCL-1 expression, suggest that MCL-1 inhibition induces a partial protective effect that resembles the decrease in apoptotic sensitivity engaged during differentiation. Consistent with this hypothesis, treatment of hESCs with GX15-070 reduced the expression of pluripotency markers NANOG and OCT4, while treatment with ABT-737 did not affect the expression of these pluripotency factors (Figures

(D) Immunofluorescence images (63×) show decreased staining for OCT4 (green) when treated with GX15-070. Nuclei: Hoechst 33258. Scale bar, 10 μm.
(E) In contrast, increasing treatments of ABT-737 do not affect OCT4 or NANOG protein levels.
(F) Treatment of hESCs with 500 nM MIM-1 results in lowered expression of NANOG and OCT4.
(G and H) Immunofluorescence (20×) shows decreased expression of NANOG and OCT4. Error bars represent ±SD for three independent experiments. Scale bar, 100 μm.
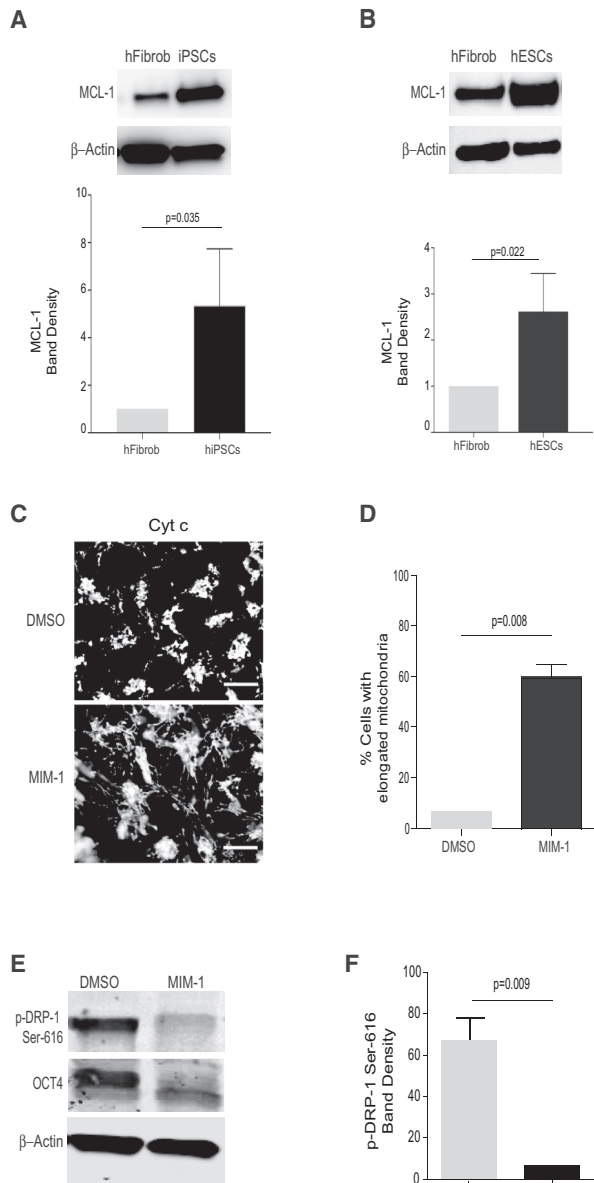See also Figure S1.

Figure 2. MCL-1 Is Highly Expressed in hESCs and Maintains Mitochondrial Fission

(A and B) MCL-1 protein expression is increased in hiPSCs (A) and hESCs (B) when compared with human fibroblasts (hFibrob). Bar graphs show quantification of band intensity relative to hFibrob β-actin.

(C) hESCs were treated with 500 nM MIM-1, inducing mitochondrial elongation. Cytochrome *c* staining (Cyt c) depicts mitochondria (63×). Scale bar, 10 μm.

(D) Quantification of cells with elongated mitochondria in (C).

(E and F) MIM-1 treatment (500 nM) in hESCs results in p-DRP-1 S616 downregulation. Band density was quantified relative to control DMSO.

All error bars represent ±SD in at least three independent experiments. See also Figure S2.

1C–1E). To confirm the effect of MCL-1 on pluripotency, we then turned to MIM-1, an MCL-1-specific small-molecule inhibitor (Cohen et al., 2012), which caused the significant decrease of both NANOG and OCT4 expression (Figures 1F–1H, S1G, and S1H). SOX2 expression was not affected by MCL-1 inhibition, suggesting that hESCs treated with MIM-1 may be differentiating to the default neuroectoderm lineage. These results indicate that MCL-1 may be necessary for hPSC maintenance of pluripotency.

MCL-1 Is Induced during Reprogramming, and Its Inhibition Causes Changes in the Stem Cell Mitochondrial Network

We next examined whether MCL-1 expression upregulation was also engaged during the transition to pluripotency. We first reprogrammed human fibroblasts by delivering pluripotency factors using the non-integrating Sendai-based vector system (Figures S2A and S2B). Compared with fibroblasts, MCL-1 is expressed at high levels in human induced PSCs (hiPSCs) (Figure 2A) and hESCs (Figure 2B), both of which are highly sensitized to cell death (Dumitru et al., 2012) (Figure S2C). Along with high expression levels of MCL-1, we also observed that iPSCs have a fragmented mitochondrial network when compared with their parent human fibroblast line (Figure S2D), consistent with previous reports suggesting that mitochondria undergo vast changes during reprogramming in response to overexpression of pluripotency factors (Chen and Chan, 2017).

We next investigated whether MCL-1 has a role in the maintenance of mitochondrial dynamics in PSCs. We inhibited MCL-1 in hESCs using MIM-1 and examined its effects on mitochondrial structure. In response to MCL-1 inhibition, the mitochondria appear to fuse and become more elongated, as shown by cytochrome *c* staining (Figures 2C and 2D). We hypothesized that these changes in mitochondrial shape could be orchestrated through cross-talk between MCL-1 and the proteins involved in mitochondrial dynamics. We first interrogated the expression levels of active DRP-1 in response to MCL-1 inhibition. Phosphorylation of DRP-1 on Ser-616 enhances DRP-1 activity (Taguchi et al., 2007). Cells treated with MIM-1 displayed downregulated DRP-1 phosphorylation (p-DRP-1 S616) compared with vehicle control cells (Figures 2E and 2F), providing evidence for a role of MCL-1 in the regulation of DRP-1 activity.

To confirm that the effects of the small-molecule inhibitor MIM-1 were due specifically to MCL-1 inhibition, we performed loss-of-function experiments utilizing an RNAi approach. MCL-1 expression was knocked down in hESCs using small interfering RNA (siRNA). As seen with the small-molecule inhibitors of MCL-1, transmission electron microscopy images confirmed significant elongation of the
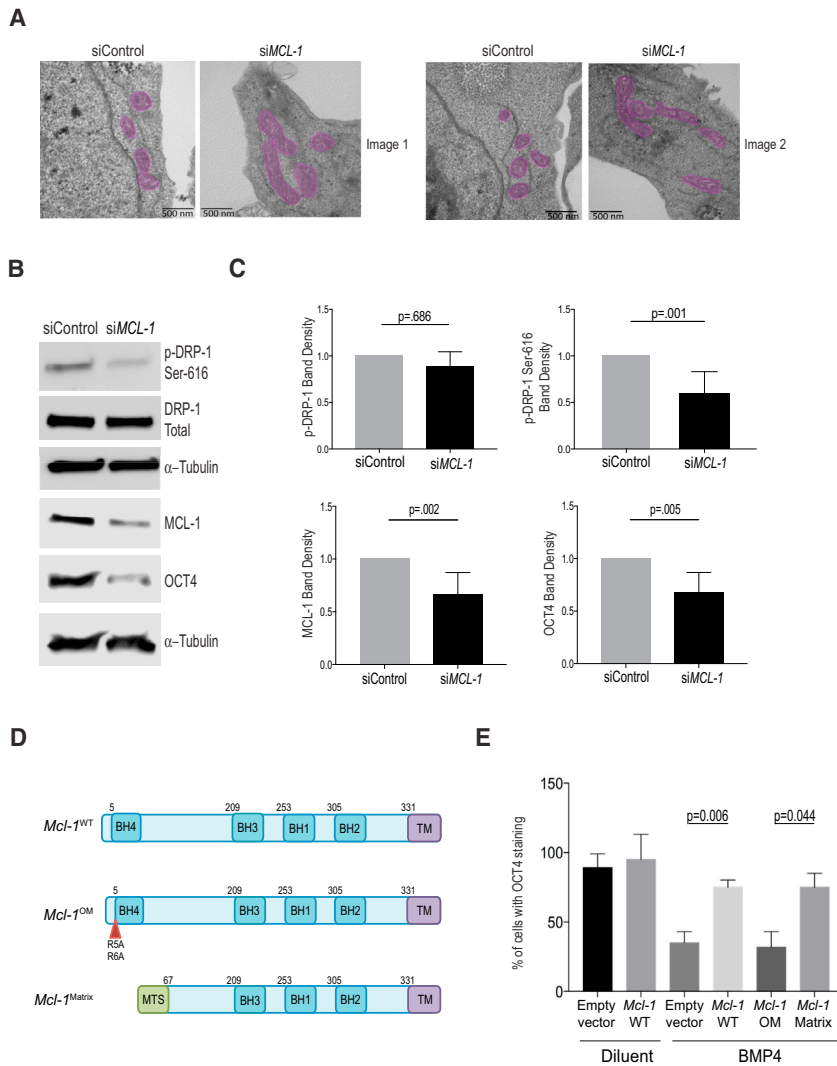
A

siControl   si*MCL-1*   siControl   si*MCL-1*

Image 1   Image 2

500 nm   500 nm   500 nm   500 nm

B

siControl   si*MCL-1*

p-DRP-1 Ser-616

DRP-1 Total

α–Tubulin

MCL-1

OCT4

α–Tubulin

C

p-DRP-1 Band Density — p=.686 — siControl / si*MCL-1*

p-DRP-1 Ser-616 Band Density — p=.001 — siControl / si*MCL-1*

MCL-1 Band Density — p=.002 — siControl / si*MCL-1*

OCT4 Band Density — p=.005 — siControl / si*MCL-1*

D

$Mcl-1^{WT}$ 5 — BH4 — 209 BH3 — 253 BH1 — 305 BH2 — 331 TM

$Mcl-1^{OM}$ 5 — BH4 — 209 BH3 — 253 BH1 — 305 BH2 — 331 TM   R5A R6A

$Mcl-1^{Matrix}$ 67 — MTS — 209 BH3 — 253 BH1 — 305 BH2 — 331 TM

E

% of cells with OCT4 staining — p=0.006 — p=0.044

Empty vector / *Mcl-1* WT | Empty vector / *Mcl-1* WT / *Mcl-1* OM / *Mcl-1* Matrix

Diluent   BMP4

Figure 3. MCL-1 Inhibition Results in Elongated Mitochondria and Low Expression of Active DRP-1

(A) Transmission electron microscopy images showing elongated mitochondrial morphology in hESCs after MCL-1 downregulation. Scale bar, 500 nm.

(B) Knockdown of MCL-1 results in lowered expression of OCT4 and p-DRP-1 S616.

(C) Quantification of western blots (WBs) in (B). Error bars represent ±SD for at least three separate experiments.

(D) Representation of murine constructs encoding MCL-1.

(E) hESCs were treated with BMP4, then transfected with $Mcl-1^{WT}$, $Mcl-1^{OM}$, or $Mcl-1^{Matrix}$. OCT4 expression was quantitated. Error bars represent ±SD for three independent experiments.
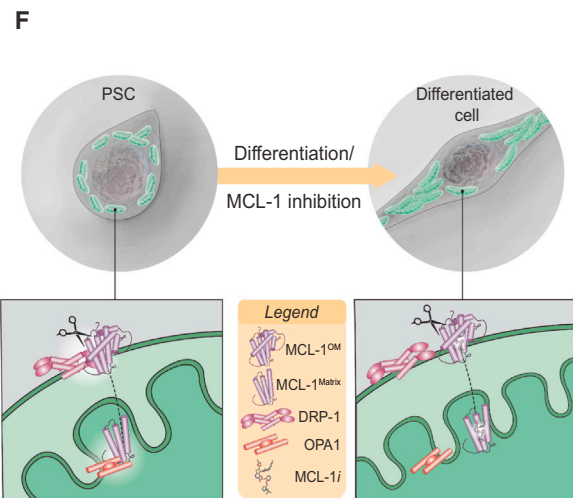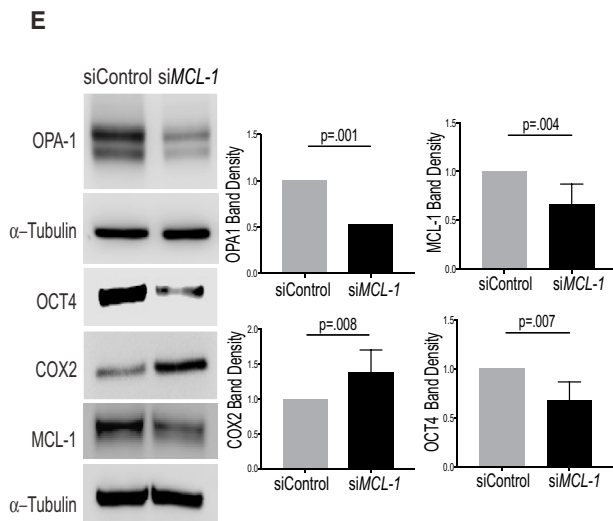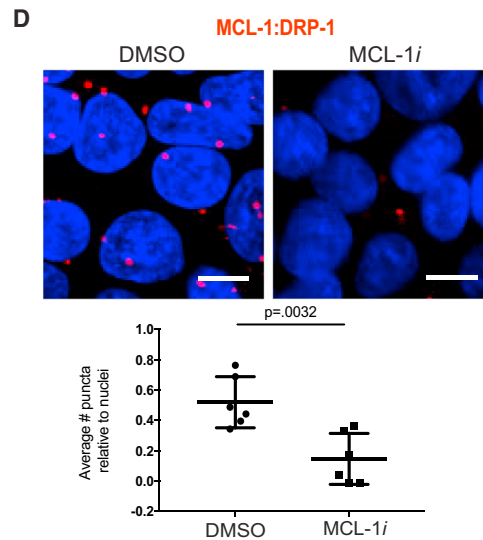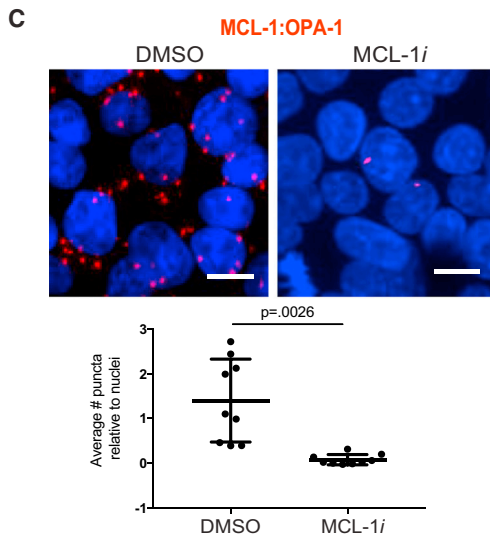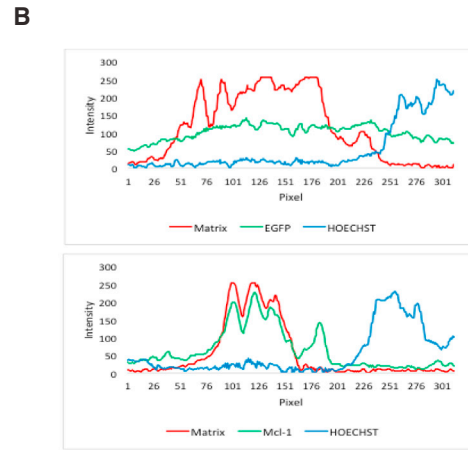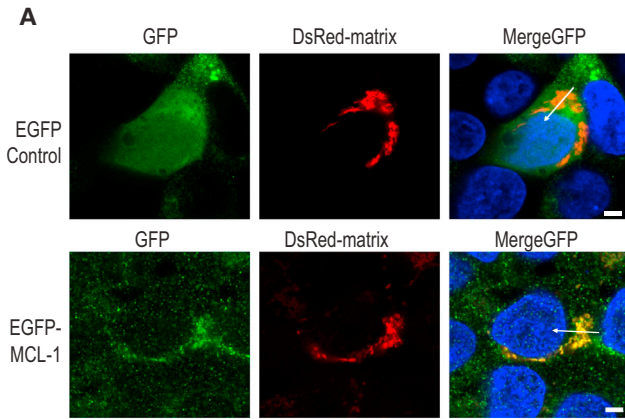
See also Figure S3.

mitochondria in MCL-1 knockdown hESCs in comparison with scramble siRNA controls (Figure 3A). Importantly, OCT4 and p-DRP-1 Ser-616 levels were also significantly decreased upon MCL-1 knockdown (Figures 3B and 3C), as seen in the presence of MIM-1. Therefore, MCL-1 appears to affect pluripotency, at least in part, through the regulation of DRP-1 activity.

Expression of MCL-1 at the Mitochondrial Matrix Delays Differentiation

It has been shown that MCL-1, besides localizing to the outer mitochondrial membrane, also localizes to the mitochondrial matrix in mouse embryonic fibroblasts and some human cancer lines. The mitochondrial targeting sequence of MCL-1 resides in an N-terminal region that is cleaved from the wild-type form, allowing MCL-1 to be trafficked into the matrix. We investigated the effect of these separate

forms of MCL-1 on maintaining pluripotency encoded by three expression vectors (Figure 3D) (Perciavalle et al., 2012): wild-type *Mcl-1* ($Mcl-1^{WT}$), mitochondrial outer membrane-located *Mcl-1* ($Mcl-1^{OM}$), and mitochondrial matrix-located *Mcl-1* ($Mcl-1^{Matrix}$). $MCL-1^{WT}$ localizes to both the outer mitochondrial membrane and the matrix. $MCL-1^{OM}$ was obtained by mutating the arginine residues at positions 5 and 6 of MCL-1 to alanine. $MCL-1^{OM}$ localizes to the mitochondrial outer membrane, preserving MCL-1 anti-apoptotic function, but it cannot be imported to the mitochondrial matrix. $MCL-1^{Matrix}$ was obtained by fusing the mitochondrial targeting sequence of matrix-localized ATP synthase to N-truncated MCL-1 (lacking the first 66 amino acids). $MCL-1^{Matrix}$ localizes exclusively to the mitochondrial matrix.

Ectopic expression of $MCL-1^{OM}$ showed the expected decrease in OCT4 expression in response to BMP4

A

GFP | DsRed-matrix | MergeGFP

EGFP Control

GFP | DsRed-matrix | MergeGFP

EGFP-MCL-1

B

C

MCL-1:OPA-1

DMSO | MCL-1*i*

p=.0026

D

MCL-1:DRP-1

DMSO | MCL-1*i*

p=.0032

E

siControl   si*MCL-1*

OPA-1
α–Tubulin
OCT4
COX2
MCL-1
α–Tubulin

OPA1 Band Density — p=.001
MCL-1 Band Density — p=.004
COX2 Band Density — p=.008
OCT4 Band Density — p=.007

F

PSC → Differentiation/ MCL-1 inhibition → Differentiated cell

Legend
MCL-1^OM
MCL-1^Matrix
DRP-1
OPA1
MCL-1*i*

(legend on next page)

(Figure 3E). Interestingly both MCL-1^{WT} and MCL-1^{Matrix} caused a delay in differentiation in response to BMP4, as shown by a decrease in OCT4-negative cells (Figures 3E and S3). These results indicate that MCL-1 may have an alternative function at the mitochondrial matrix in maintaining pluripotency.

MCL-1 Interacts with and Maintains the Stability of DRP-1 and OPA1

To confirm that MCL-1 is in fact localized to the mitochondrial matrix in hPSCs, we co-expressed a GFP-tagged *MCL-1* construct (EGFP-MCL-1) and a DsRed-mito construct, which encodes a truncated form of cytochrome *c* oxidase subunit 2 (COX2) that localizes exclusively to the mitochondrial matrix (Figure 4A). Line-scan measurements of fluorescence show that MCL-1 co-localizes with the matrix marker, DsRed-mito (Figure 4B). The localization of MCL-1 at both the outer mitochondrial membrane and at the matrix in stem cells suggests that MCL-1 could be interacting with DRP-1 (at the outer membrane) to promote mitochondrial fragmentation and/or OPA1 (at the matrix) to repress fusion of the mitochondrial network in hESCs.

To test this possibility, we performed co-immunoprecipitation experiments using both total cell fractions and mitochondrial purifications to pull down MCL-1 and check for binding to DRP-1 and OPA1 (Figure S4A). Western blot analysis identified a shifted band roughly 20 kDa larger than the expected DRP-1 band (Figure S4B). We speculate that this could be a modified, active form of DRP-1, presumably due to its phosphorylation and sumoylation when in its active state (Anderson and Blackstone, 2013; Chang and Blackstone, 2010). In the total cell fraction, we did not detect binding between MCL-1 and OPA1. However, we detected strong binding in mitochondrial preparations of hESCs (Figure S4B). These *in vitro* biochemical assays suggest that MCL-1 is binding to both DRP-1 and OPA1 in human embryonic stem cells.

We then used a proximity ligation assay (PLA) to confirm binding of these proteins *in situ* (Figure S4C). We first confirmed MCL-1 interaction to the BH3-only protein, BIM. BIM is known to bind MCL-1 by inserting its BH3 domain into MCL-1's surface groove (Martinou and Youle, 2011). We detected the expected interaction of MCL-1 and BIM, as indicated by red fluorescent puncta (Figure S4D). We then probed for binding of MCL-1 with both OPA1 and DRP-1. Indeed, as seen in the immunoprecipitation experiments, we detected MCL-1 interaction with OPA1 (Figure 4C) and DRP-1 (Figure 4D). We then used a derivative of a recently reported MCL-1 inhibitor, S63845 (Kotschy et al., 2016), which works by competing for binding to the BH3 domain of MCL-1. We confirmed that S63845 also caused changes to the mitochondrial network (Figure S4E). As expected, S63845 effectively disrupted the interaction between MCL-1 and BIM (Figure S4D). Interestingly, as indicated by the decrease in the number of puncta, S63845 (MCL-1*i*) disrupts interactions with mitochondrial dynamics machinery at both the outer mitochondrial membrane (MCL-1:DRP-1) and the matrix (MCL-1:OPA1) (Figures 4C and 4D). These results suggest that MCL-1 associates with both GTPases through its characteristic hydrophobic binding groove (Billard, 2013).

Previously, we determined that MCL-1 downregulation affected the activity of DRP-1, but not its stability (Figure 3B). Interestingly, MCL-1 downregulation did cause a significant decrease in OPA1 expression (Figure 4E), indicating that MCL-1 influences OPA1 stability, but not necessarily its function, since the mitochondria in hESCs are still capable of fusing when MCL-1 is inhibited (Figure 3A). Mitochondrial fusion is key for efficient assembly of the electron transport chain (ETC). Interestingly, OPA1 has also been implicated in maintaining oxidative phosphorylation in cells. Thus, our results suggest that preventing OPA1 activity (either in fusion or in OXPHOS) could be crucial for maintaining stem cell pluripotency.

Taken together, our findings imply that MCL-1 modulates mitochondrial dynamics and pluripotency through interactions with mitochondrial fission and fusion regulators. Based on our observations, we propose a model in which MCL-1 at the outer mitochondrial membrane regulates cell death and promotes DRP-1 activity and

Figure 4. MCL-1 Regulates Mitochondrial Dynamics through Interaction with DRP-1 and OPA1
(A) hiPSCs expressing EGFP-MCL-1 or control EGFP and DsRed-mito. Scale bar, 2 μm.
(B) Fluorescence intensity plots show co-localization of EGFP-MCL-1 and DsRed-mito. Arrow indicates location of the line used for fluorescence intensity by line scan.
(C and D) PLA of cells treated for 6 hr with or without 100 nM S63845 (MCL-1*i*). Representative Z-stack images are shown. Red indicates MCL-1:OPA1 (C) and MCL-1:DRP-1 (D) proximity; blue indicates Hoechst 33258. Average puncta/cell was quantitated for at least 300 cells/sample (each sample done in triplicate). Error bars represent ±SEM from three independent experiments, Welch's unpaired 2-tailed t test. Scale bar, 10 μm.
(E) Western blot of MCL-1 after siRNA-mediated knockdown. At least three independent experiments were quantified. Error bars represent ±SD.
(F) Working model of MCL-1 regulation of mitochondrial dynamics.
See also Figure S4.

mitochondrial fragmentation (Figure 4F). Our results with S63845 (Letai, 2016) suggest that these interactions are modulated through the MCL-1 BH3 binding groove. It would be interesting to test whether there are two pools of MCL-1, one that is binding to the pro-apoptotic proteins and inhibiting apoptosis and another capable of binding and regulating DRP-1, promoting mitochondrial fragmentation. It will also be necessary to follow up the effects of MCL-1 inhibition-induced mitochondrial changes on the metabolic state of PSCs. In addition, examining the metabolic requirement for MCL-1 during reprogramming could be intriguing in light of recent reports suggesting a multistage reprogramming process (Lee et al., 2016).

The process of differentiation into progenitors and committed cells is likely regulated, at least in part, by a shift in dependence to MCL-1 anti-apoptotic activity. It will be crucial to examine MCL-1's function in adult stem cells from different tissues. Likewise, identifying the signaling pathways by which mitochondria-nucleus crosstalk occurs upstream and downstream of MCL-1 in stem cells and their progenitors, as has been shown with murine neural progenitor cells (Khacho et al., 2016), is an important future direction. By studying the role of MCL-1 in mitochondrial dynamics, we can increase our understanding of the fundamental mechanisms governing pluripotency and self-renewal.

EXPERIMENTAL PROCEDURES

A detailed description of all methods is included in the Supplemental Information.

Cell Culture
H9 hESC line was obtained from WiCell. All experiments with pluripotent stem cells were performed under the supervision of the Vanderbilt Institutional Human Pluripotent Cell Research Oversight (VIHPCRO) Committee. Details of stem cell culture maintenance and treatments are described in Supplemental Experimental Procedures.

Transfections
Commercially available siRNA was used to knock down MCL-1 using RNAi max (Thermo Fisher). For overexpression of MCL-1, GFP-tagged MCL-1, and DsRed-mito proteins, Fugene (Promega) was used. Transductions are described in Supplemental Experimental Procedures.

Binding Assays
Dynabeads (Invitrogen) were used for immunoprecipitation experiments, and the DuoLink kit (Sigma) was used for PLA.

Immunofluorescence
Cells were fixed with 4% paraformaldehyde and processed as described in Supplemental Experimental Procedures.

SUPPLEMENTAL INFORMATION

Supplemental Information includes Supplemental Experimental Procedures, four figures, and two tables and can be found with this article online at https://doi.org/10.1016/j.stemcr.2018.01.005.

AUTHOR CONTRIBUTIONS

V.G. and M.L.R. designed experiments. M.L.R., K.P.P., N.A.O., C.C.A., A.I.R.-M., L.A.K., K.E.B., and V.G. performed experiments and analyzed data. M.L.R. and V.G. wrote the manuscript.

REFERENCES

Amita, M., Adachi, K., Alexenko, A.P., Sinha, S., Schust, D.J., Schulz, L.C., Roberts, R.M., and Ezashi, T. (2013). Complete and unidirectional conversion of human embryonic stem cells to trophoblast by BMP4. Proc. Natl. Acad. Sci. USA *110*, E1212–E1221.

Andersen, J.L., and Kornbluth, S. (2012). Mcl-1 rescues a glitch in the matrix. Nat. Cell Biol. *14*, 563–565.

Anderson, C.A., and Blackstone, C. (2013). SUMO wrestling with Drp1 at mitochondria. EMBO J. *32*, 1496–1498.

Billard, C. (2013). BH3 mimetics: status of the field and new developments. Mol. Cancer Ther. *12*, 1691–1700.

Chambers, S.M., Fasano, C.A., Papapetrou, E.P., Tomishima, M., Sadelain, M., and Studer, L. (2009). Highly efficient neural conversion of human ES and iPS cells by dual inhibition of SMAD signaling. Nat. Biotechnol. *27*, 275–280.

Chang, C.R., and Blackstone, C. (2010). Dynamic regulation of mitochondrial fission through modification of the dynamin-related protein Drp1. Ann. N. Y. Acad. Sci. *1201*, 34–39.

Chen, H., and Chan, D.C. (2017). Mitochondrial dynamics in regulating the unique phenotypes of cancer and stem cells. Cell Metab. *26*, 39–48.

Chen, H., and Chan, D.C. (2010). Physiological functions of mitochondrial fusion. Ann. N. Y. Acad. Sci. *1201*, 21–25.

Chiappori, A.A., Schreeder, M.T., Moezi, M.M., Stephenson, J.J., Blakely, J., Salgia, R., Chu, Q.S., Ross, H.J., Subramaniam, D.S., and Berger, M.S. (2012). A phase I trial of pan-Bcl-2 antagonist obatoclax administered as a 3-h or a 24-h infusion in combination with carboplatin and etoposide in patients with extensive-stage small cell lung cancer. Br. J. Cancer *106*, 839–845.

Cohen, N.A., Stewart, M.L., Gavathiotis, E., Tepper, J.L., Bruekner, S.R., Koss, B., Opferman, J.T., and Walensky, L.D. (2012). A competitive stapled peptide screen identifies a selective small molecule that overcomes MCL-1-dependent leukemia cell survival. Chem. Biol. *19*, 1175–1186.

Dumitru, R., Gama, V., Fagan, B.M., Bower, J.J., Swahari, V., Pevny, L.H., and Deshmukh, M. (2012). Human embryonic stem cells have constitutively active Bax at the Golgi and are primed to undergo rapid apoptosis. Mol. Cell *46*, 573–583.

Friedman, J.R., and Nunnari, J. (2014). Mitochondrial form and function. Nature *505*, 335–343.

Karbowski, M., Lee, Y.J., Gaume, B., Jeong, S.Y., Frank, S., Nechushtan, A., Santel, A., Fuller, M., Smith, C.L., and Youle, R.J. (2002). Spatial and temporal association of Bax with mitochondrial fission sites, Drp1, and Mfn2 during apoptosis. J. Cell Biol. *159*, 931–938.

Karbowski, M., Norris, K.L., Cleland, M.M., Jeong, S.Y., and Youle, R.J. (2006). Role of Bax and Bak in mitochondrial morphogenesis. Nature *443*, 658–662.

Khacho, M., Clark, A., Svoboda, D.S., Azzi, J., MacLaurin, J.G., Meghaizel, C., Sesaki, H., Lagace, D.C., Germain, M., Harper, M.E., et al. (2016). Mitochondrial dynamics impacts stem cell identity and fate decisions by regulating a nuclear transcriptional program. Cell Stem Cell *19*, 232–247.

Kotschy, A., Szlavik, Z., Murray, J., Davidson, J., Maragno, A.L., Le Toumelin-Braizat, G., Chanrion, M., Kelly, G.L., Gong, J.N., Moujalled, D.M., et al. (2016). The MCL1 inhibitor S63845 is tolerable and effective in diverse cancer models. Nature *538*, 477–482.

Kumar, R.M., Cahan, P., Shalek, A.K., Satija, R., DaleyKeyser, A., Li, H., Zhang, J., Pardee, K., Gennert, D., Trombetta, J.J., et al. (2014). Deconstructing transcriptional heterogeneity in pluripotent stem cells. Nature *516*, 56–61.

Lee, M.R., Mantel, C., Lee, S.A., Moon, S.H., and Broxmeyer, H.E. (2016). MiR-31/SDHA axis regulates reprogramming efficiency through mitochondrial metabolism. Stem Cell Reports *7*, 1–10.

Letai, A. (2016). S63845, an MCL-1 selective BH3 mimetic: another arrow in our quiver. Cancer Cell *30*, 834–835.

Liu, J.C., Guan, X., Ryan, J.A., Rivera, A.G., Mock, C., Agarwal, V., Letai, A., Lerou, P.H., and Lahav, G. (2013). High mitochondrial priming sensitizes hESCs to DNA-damage-induced apoptosis. Stem Cell *13*, 483–491.

Llambi, F., Moldoveanu, T., Tait, S.W.G., Bouchier-Hayes, L., Temirov, J., McCormick, L.L., Dillon, C.P., and Green, D.R. (2011). A unified model of mammalian BCL-2 protein family interactions at the mitochondria. Mol. Cell *44*, 517–531.

Longo, D.L., and Archer, S.L. (2013). Mitochondrial dynamics—mitochondrial fission and fusion in human diseases. N. Engl. J. Med. *369*, 2236–2251.

Martinou, J.C., and Youle, R.J. (2011). Mitochondria in apoptosis: Bcl-2 family members and mitochondrial dynamics. Dev. Cell *21*, 92–101.

Ni Chonghaile, T., and Letai, A. (2008). Mimicking the BH3 domain to kill cancer cells. Oncogene *27* (*Suppl 1*), S149–S157.

Odorico, J.S., Kaufman, D.S., and Thomson, J.A. (2001). Multilineage differentiation from human embryonic stem cell lines. Stem Cells *19*, 193–204.

Oltersdorf, T., Elmore, S.W., Shoemaker, A.R., Armstrong, R.C., Augeri, D.J., Belli, B.A., Bruncko, M., Deckwerth, T.L., Dinges, J., Hajduk, P.J., et al. (2005). An inhibitor of Bcl-2 family proteins induces regression of solid tumours. Nature *435*, 677–681.

Opferman, J.T. (2015). Attacking cancer's Achilles heel: antagonism of anti-apoptotic BCL-2 family members. FEBS J. *283*, 2661–2675.

Perciavalle, R.M., Stewart, D.P., Koss, B., Lynch, J., Milasta, S., Bathina, M., Temirov, J., Cleland, M.M., Pelletier, S., Schuetz, J.D., et al. (2012). Anti-apoptotic MCL-1 localizes to the mitochondrial matrix and couples mitochondrial fusion to respiration. Nat. Cell Biol. *14*, 575–583.

Prieto, J., León, M., Ponsoda, X., Sendra, R., Bort, R., Ferrer-Lorente, R., Raya, A., López-García, C., and Torres, J. (2016). Early ERK1/2 activation promotes DRP1-dependent mitochondrial fission necessary for cell reprogramming. Nat. Commun. *7*, 11124.

Ramalho-Santos, M., Yoon, S., Matsuzaki, Y., Mulligan, R.C., and Melton, D.A. (2002). "Stemness": transcriptional profiling of embryonic and adult stem cells. Science *298*, 597–600.

Rinkenberger, J.L., Horning, S., Klocke, B., Roth, K., and Korsmeyer, S.J. (2000). Mcl-1 deficiency results in peri-implantation embryonic lethality. Genes Dev. *14*, 23–27.

Sheridan, C., Delivani, P., Cullen, S.P., and Martin, S.J. (2008). Bax- or Bak-induced mitochondrial fission can be uncoupled from cytochrome C release. Mol. Cell *31*, 570–585.

Taguchi, N., Ishihara, N., Jofuku, A., Oka, T., and Mihara, K. (2007). Mitotic phosphorylation of dynamin-related GTPase Drp1 participates in mitochondrial fission. J. Biol. Chem. *282*, 11521–11529.

Wai, T., and Langer, T. (2016). Mitochondrial dynamics and metabolic regulation. Trends Endocrinol. Metab. *27*, 105–117.

Westermann, B. (2010). Mitochondrial fusion and fission in cell life and death. Nat. Rev. Mol. Cell Biol. *11*, 872–884.